



**HAL**  
open science

# ftz-f1 and Hr39 opposing roles on EcR expression during Drosophila mushroom body neuron remodeling

Ana Boulanger, Jean-Maurice Dura

## ► To cite this version:

Ana Boulanger, Jean-Maurice Dura. ftz-f1 and Hr39 opposing roles on EcR expression during Drosophila mushroom body neuron remodeling. *Nature Neuroscience*, 2010, 10.1038/nn.2700 . hal-00598184

**HAL Id: hal-00598184**

**<https://hal.science/hal-00598184>**

Submitted on 5 Jun 2011

**HAL** is a multi-disciplinary open access archive for the deposit and dissemination of scientific research documents, whether they are published or not. The documents may come from teaching and research institutions in France or abroad, or from public or private research centers.

L'archive ouverte pluridisciplinaire **HAL**, est destinée au dépôt et à la diffusion de documents scientifiques de niveau recherche, publiés ou non, émanant des établissements d'enseignement et de recherche français ou étrangers, des laboratoires publics ou privés.

***ftz-f1* and *Hr39* opposing roles on *EcR* expression during *Drosophila* mushroom body neuron remodeling**

**Ana Boulanger<sup>1</sup>, Christelle Clouet-Redt<sup>1</sup>, Morgane Farge<sup>1</sup>, Adrien Flandre<sup>1</sup>, Thomas Guignard<sup>1</sup>, Céline Fernando<sup>2</sup>, François Juge<sup>2</sup> and Jean-Maurice Dura<sup>1</sup>**

<sup>1</sup>Institute of Human Genetics

CNRS UPR1142

141, rue de la Cardonille,

34396 Montpellier Cedex 5 France

<sup>2</sup> Institut de Génétique Moléculaire de Montpellier, UMR 5535 CNRS, 1919 Route de Mende, 34293 Montpellier Cedex 5 France. Université Montpellier 2, Place Eugène Bataillon, 34095 Montpellier cedex 5. Université Montpellier 1, 5 Bd Henry IV, 34967 Montpellier cedex 2.

A.B. and C.C.-R. contributed equally to this work.

Correspondence should be addressed to J.-M. D. ([jmdura@igh.cnrs.fr](mailto:jmdura@igh.cnrs.fr))

## Summary

Developmental axon pruning is a general mechanism required for maturation of neural circuits. During *Drosophila* metamorphosis, the larval-specific dendrites and axons of early  $\gamma$  neurons of the mushroom bodies are pruned and replaced by adult-specific processes. We show here that the nuclear receptor *ftz-f1* is required for this pruning and has two roles: (i) to activate expression of the steroid hormone receptor *EcR-B1* whose activity is essential for  $\gamma$  remodeling and (ii) to repress expression of *Hr39*, a *ftz-f1* homologous gene. If inappropriately expressed in the  $\gamma$  neurons, HR39 inhibits normal pruning likely by competing with endogenous FTZ-F1 that results in decreased *EcR-B1* expression. *EcR-B1* was previously identified as a target of the TGF- $\beta$  signaling pathway. Here we show that the *ftz-f1/Hr39* pathway acts apparently independent from TGF- $\beta$  signaling, suggesting that *EcR-B1* is the target of two parallel molecular pathways acting during  $\gamma$  neuron remodeling.

## Introduction

During nervous system development in both vertebrates and invertebrates, neurons undergo a remodeling process which is necessary for their normal function<sup>1,2</sup>. This neuronal remodeling involves dendrite and axon pruning which leaves the morphology of the neuronal cell body unaffected. A well documented case of neuronal remodeling is the developmental axon pruning of mushroom bodies  $\gamma$  neurons that occurs during metamorphosis in *Drosophila*<sup>3-10</sup>. The mushroom bodies are a bilaterally-symmetric structure in the larval and adult brain. Each adult mushroom body is comprised of  $\sim 2,000$  neurons which arise from four neuroblasts<sup>11</sup>. These neurons project their axons into two vertical lobes ( $\alpha$  and  $\alpha'$ ) and three medial lobes ( $\beta$ ,  $\beta'$  and  $\gamma$ ). Each neuroblast generates three distinct classes of neurons with axonal projections

in different lobes in a sequential fashion <sup>12</sup>, specifically the  $\gamma$  neurons (late embryonic and early larval stage),  $\alpha'\beta'$  neurons (late larval stage) and  $\alpha\beta$  neurons (pupal stage). The  $\gamma$  neurons are the first to arise, and undergo pruning of larval-specific dendrites and axons at metamorphosis. This pruning is followed by re-growth of adult specific dendrites and axons. Notably, although larval  $\gamma$  neurons have branched axons projecting into both dorsal and medial lobes, the adult  $\gamma$  axons do not bifurcate and thus project only into the single medial  $\gamma$  lobe <sup>3</sup>.

In insects, maturation at metamorphosis is regulated by the steroid hormone 20-hydroxyecdysone (hereafter called ecdysone). Ecdysone binds a heterodimeric nuclear receptors formed by the interaction of the ecdysone receptor (ECR) and the product of *ultraspiracle*, USP. Neuronal remodeling in *Drosophila* is controlled, at least in part, by steroid receptors <sup>13, 14</sup>. In particular, a cell-autonomous role for ECR/USP in controlling  $\gamma$  neuron remodeling is described <sup>3</sup>. Phylogenetic analysis of nuclear receptor genes reveals six distinct subfamilies. Subfamily five includes FTZ-F1 and HR39 together with the human homologues SF1 (steroidogenic factor 1) and closely related LRH1 (liver receptor homologue 1) <sup>15</sup>. The nuclear receptor gene *Hr39* has high sequence similarity to *ftz-fl*. Both *ftz-fl* and *Hr39* are expressed post-embryonically and particularly at the pre-pupal stage <sup>15-18</sup>. *Hr39* expression is apparently down-regulated at time points when *ftz-fl* expression reaches maximum levels. Moreover, both receptors bind *in vitro* the same site in the *Alcohol dehydrogenase (Adh)*, *fushi tarazu (ftz)* and *new glue (ng)* gene <sup>19-21</sup>. Opposing *in vitro* transcriptional activity is reported in the corresponding common binding sites. Therefore, *in vivo* functional competition of these two nuclear receptors on common target-gene transcription is likely. We show here that *ftz-fl* was required for  $\gamma$  neuron remodeling by activating *EcR-B1* and repressing *Hr39*.

## RESULTS

### ***βftz-f1* function is required for $\gamma$ neuron pruning**

To investigate a possible requirement of *ftz-f1* wild-type function in mushroom body remodeling we examined  $\gamma$  neuron pruning in the well-characterized null mutant *ftz-f1<sup>ex7</sup>* background<sup>17, 22</sup>. In the adult mushroom bodies, the *GAL4-201Y* enhancer trap is expressed both in  $\gamma$  neurons and a small subset of  $\alpha\beta$  neurons called the  $\alpha\beta$ -core<sup>12, 23-25</sup>. Since loss of global *ftz-f1* activity results in embryonic lethality, we used *GAL4-201Y* in the mosaic analysis with the repressible cell marker (MARCM) system and identified neuroblast and single-cell  $\gamma$  neuron homozygous mutant clones in adults. They were induced in newly hatched larvae and subsequently visualized with a membrane-targeted GFP marker<sup>24</sup>. The *ftz-f1<sup>ex7</sup>* mutant  $\gamma$  neuron neuroblast clones (n = 28) retained their larval-type branching of axons into the adult stage (**Fig. 1** and **Table 1a**). The mutant phenotype could also be seen in single/two cell clones (**Fig. 1e**). Thirty single *ftz-f1<sup>-/-</sup>* clones were analyzed: 24 were wild-type (80%) and 6 were un-pruned (20%). The wild type appearance of the majority of the single clones indicates a high level of perdurance of the wild-type *ftz-f1* product. As control, 21 single *+/+* clones were analyzed and 100% were wild-type. As expected, the *ftz-f1<sup>ex7</sup>* neuroblast clones were indistinguishable from wild-type at the third larval stage, but displayed no signs of pruning at 24 h after puparium formation (APF) in contrast to their wild-type counterparts in which most axons were fully pruned (data not shown). This mutant axon remodeling phenotype was essentially completely rescued (**Fig. 1f** and **Table 1a**). These results demonstrated a cell-autonomous requirement for *βftz-f1* activity during metamorphosis for the majority of  $\gamma$  neurons to be appropriately pruned.

FTZ-F1 is detected in early second instar but not in late second or third instar larvae<sup>17</sup>. We therefore localized FTZ-F1 in the second instar larval brain by anti-FTZ-F1

immunostaining<sup>17,26</sup>. FTZ-F1 protein was found to be ubiquitously expressed including in the  $\gamma$  neuron cell bodies which were identified by their expression of GFP under the control of the *GAL4-201Y* driver (**Supplementary Fig. 1**). A definitive control of the specificity of the anti-FTZ-F1 antibody would be to show the lack of FTZ-F1 expression in *ftz-fl<sup>-/-</sup>* MARCM second instar larval clones. Unfortunately, we were not able to produce such clones, very likely due to the short period of time between transposase-mediated mitotic recombination and the stage at which we could identify clones.

### **Over-expression of the *Hr39* blocks $\gamma$ neuron remodeling**

FTZ-F1 and HR39 bind to identical DNA sequences and have opposing *in vitro* transcriptional activity indicating a potential functional antagonism<sup>19-21</sup>. Therefore, we reasoned that if the *ftz-fl* lack-of-function (LOF) blocks  $\gamma$  axon pruning, then the gain-of-function (GOF) of *Hr39* would do the same. We took three different approaches to over-express *Hr39* to establish a GOF. First, we replaced the original *P{GawB}* element present in the *GAL4-c739* enhancer trap line and located within the *Hr39* transcriptional unit 9.5 kb upstream of the ATG start codon, with the *P{Mae-UAS.6.11}*, thereby placing the endogenous *Hr39* gene under UAS control<sup>23,27</sup> (*Hr39<sup>Cl3</sup>*). Furthermore, we identified a UAS-bearing *P*-element insertion located 1.5 kb upstream of *Hr39*'s initiator ATG codon, *P{GS:9939}*, in the Kyoto stock collection (DGRC). Both UAS insertions were shown to express *Hr39* by RT-PCR when driven by the *GAL4-OK107* mushroom body driver (data not shown). Finally we generated UAS lines bearing a full length *Hr39* cDNA transgene.

Ectopic expression of all three HR39 GOFs, driven by *GAL4-201Y* in developing  $\gamma$  neurons blocked pruning resulting in similar mutant phenotypes (**Fig. 2**). Although some  $\gamma$  neurons seemed normally pruned, 100% of the mushroom bodies (n > 20) predominantly

displayed  $\gamma$  neurons which retained their larval characteristics (**Fig. 2d** and **Table 1b**). As expected from the mode of action of a nuclear receptor, the un-pruned phenotype induced by HR39 ectopic expression was cell-autonomous as determined by MARCM experiments. In the mutant neuroblast clones there was a mixture of un-pruned and apparently pruned  $\gamma$  neurons, reproducing what we observed in fully mutant mushroom bodies (**Fig. 2e**). Similarly, in two two-cell mutant clones, two mutant neurons were clearly un-pruned while two others appeared normal (**Fig. 2f**). Finally, our results showed that only  $\gamma$  neurons seemed affected by *Hr39* ectopic expression in adult mushroom body neurons (**Supplementary Figs. 2 and 3**). In conclusion, *Hr39* over-expression in the mushroom body produced a cell-autonomous blockade of the  $\gamma$  neuron remodeling. In the mushroom body, FTZ-F1 and HR39 homologous nuclear receptors seemed to have opposing functions in  $\gamma$  axon pruning. In order for normal pruning to occur, *Hr39* must be actively repressed during remodeling of the  $\gamma$  neurons as its presence interferes with this process.

### ***ftz-fl* and *Hr39* are not targets of ECR-B1 in $\gamma$ neurons**

Based on a previous study, we expected the *ftz-fl* and *Hr39* genes to be either direct or indirect targets of the ecdysone-ECR-USP complex<sup>15</sup>. We therefore hypothesized that ECR-B1 activates *ftz-fl* and represses *Hr39* transcription. In order to test this hypothesis, we first had to produce a definitely null *Hr39* allele. The *Hr39* mutations previously described all bear insertions of *P* elements in the *Hr39* transcriptional unit which do not disrupt the open reading frame, and may thus not be null alleles<sup>28,29</sup>. After imprecise excision of the *P*{*GS:9939*} *P*-element insertion, we recovered *Hr39*<sup>C105</sup>, which bears a homozygous viable deletion of ~ 8 kb in the transcriptional unit which extends into the open reading frame (**Fig. 2g**). In addition, we confirmed the null status of *Hr39*<sup>C105</sup> by immunoblotting wild-type versus mutant head

extract proteins with an anti-HR39 antibody (**Fig. 2h**). *Hr39*<sup>C105</sup> individuals show normal  $\gamma$  axon pruning but display  $\alpha\beta$  axon defects (see below).

It is not possible to directly produce *EcR-B1* mutant cell clones as the *EcR* locus (42A2-12) is situated between the centromere and the available more proximal FRT insertions (42B). Nevertheless, because ECR acts in a complex with another nuclear receptor, USP, functional loss of *EcR* can be established in *usp* mutant cell clones<sup>3</sup>. If the hypothesis that ECR-B1 activates *ftz-fl* and represses *Hr39* transcription was correct then it should have been possible to rescue blocked neuronal remodeling in *usp*<sup>-/-</sup> neuroblast clones if they simultaneously express wild-type  $\beta$ FTZ-F1 protein and are devoid of any *Hr39* function. However, no rescue was obtained in such neuroblast clones (**Table 1e**). This suggests that *EcR-B1* does not act upstream of *ftz-fl* and *Hr39*.

### ***EcR-B1* is a target of FTZ-F1 and HR39 in $\gamma$ neurons**

Many transcriptional targets of the ecdysone-ECR-USP complex are themselves nuclear-receptor superfamily members. Despite being *a priori* less likely, the results obtained with *ftz-fl* LOF and *Hr39* GOF could be interpreted in an alternative fashion. Specifically, *EcR-B1* expression may be up-regulated by FTZ-F1 and down-regulated by HR39 if the latter is ectopically expressed in the  $\gamma$  neurons. Two observations support this hypothesis. First, FTZ-F1 binds the polytene chromosome band 42A where *EcR* is located<sup>30</sup>. Second, at 10 h APF, the expression of *EcR* is reduced in *hs-ftz-fl* RNAi individuals after heat shock<sup>31</sup>. If this hypothesis is correct, expressing ECR-B1 in *ftz-fl* LOF clones or *Hr39* GOF mushroom bodies should restore normal  $\gamma$  neuron remodeling. This was found to be the case (**Fig. 3** and **Table 1a, b**). Furthermore, the level of ECR-B1 expression in  $\gamma$  neurons in *ftz-fl* LOF and *Hr39* GOF mutant clones and mushroom body should be reduced or even abolished. This was what we observed (**Fig. 4**). We consistently detected high levels of ECR-B1 immunostaining

in wild-type clones (n = 10) and mushroom bodies (n = 19) while ECR-B1 was essentially absent in mutant clones (n = 11) or mushroom bodies (n = 21).

It is established that the phenotype induced by the lack of *usp/EcR-B1* ecdysone receptor is a defect in pruning and not a cell fate alteration<sup>3</sup>. Since all the phenotypes described here were rescued by forced ECR-B1 expression it seems very unlikely that *ftz-fl/Hr39* controls neuronal subtype specification (see also **Supplementary Figs. 2–6bis**).

### **Two independent pathways during $\gamma$ neuron remodeling**

*EcR-B1*, whose activity is required for  $\gamma$  neuron remodeling, is a target of the TGF- $\beta$  signaling pathway<sup>4</sup>. Mutations in the *babo* gene, which encodes the TGF- $\beta$ /activin type I receptor of *Drosophila*, and in *dSmad2*, its downstream transcriptional effector, block  $\gamma$  neuronal remodeling. Restoring ECR-B1 function in *babo* mutant clones partially rescues the remodeling defects.

Thus, *ftz-fl* and *Hr39* could be positive and negative targets of the TGF- $\beta$ /*babo* signaling pathway, respectively. If this was the case, we expected a rescue of the remodeling defects observed in *babo* mutant clones if they simultaneously expressed *ftz-fl* and were devoid of any *Hr39* function. However, no rescue occurred in these clones; 19 neuroblast, 5 multiple-cell and 13 single-cell clones displayed the mutant phenotype, indicating that the two pathways appeared to target *EcR-B1* expression independently (**Table 1d** and **Supplementary Fig. 7**). Additional indications that *ftz-fl/Hr39* were not downstream targets of *babo* neither *babo* being a *ftz-fl/Hr39* target are provided (**Supplementary Figs. 8–10**).

### ***Hr39* is repressed by FTZ-F1 in the remodeling $\gamma$ neurons**

As mentioned above, the *Hr39* gene must be silenced, or at least down-regulated, in the remodeling  $\gamma$  neurons for axon pruning to occur normally. We examined the possibility that

FTZ-F1 regulates *Hr39* transcription. Two direct predictions from this hypothesis would be the ability of the absence of *Hr39* to rescue non-remodeled *ftz-fl* mutant  $\gamma$  neurons and the observation of increased HR39 expression in *ftz-fl* mutant clones.

A clear, albeit partial, rescue was indeed observed in the double mutant neuroblast clones obtained (**Table 1f** and **Supplementary Fig. 11**). This phenotypic rescue is correlated to an increased ECR-B1 expression (**Supplementary Fig. 9j**). Furthermore, significantly increased cytoplasmic HR39 expression was observed in *ftz-fl* mutant clones as compared to wild-type clones (**Fig. 5d-i**). HR39 over-expression controls were stained with the anti-HR39 antibody to demonstrate its specificity (**Supplementary Fig. 12**). Together, these data indicate that FTZ-F1 regulates *Hr39* expression, keeping it in check during  $\gamma$  neuron remodeling.

### **Antagonism between FTZ-F1 and HR39 for $\gamma$ remodeling**

Ectopic expression of *Hr39* in  $\gamma$  neurons altered normal axon pruning likely by reducing ECR-B1 levels (**Fig. 4**). Similarly, the absence of FTZ-F1 was associated with a lack of or a reduction in ECR-B1 levels, in part due to increased *Hr39* expression. Therefore, one possibility is that a functional competition may exist between the two homologous nuclear receptors FTZ-F1 and HR39 for regulating the *EcR-B1* gene. We attempted to rescue pruning in  $\gamma$  neurons ectopically expressing HR39 by over-expressing FTZ-F1. The defects observed when *UAS-Hr39* was over-expressed in the  $\gamma$  neurons (**Fig. 2**) were indeed partially rescued by simultaneous expression of the *UAS- $\beta$ ftz-fl* transgene (**Fig. 5j-l** and **Table 1c**). ECR-B1 expression is also rescued in this context (**Supplementary Fig. 9a-e**), indicating a correlation between ECR-B1 expression and phenotypic pruning level.

The mutant pruning phenotype induced by ectopic expression of *Hr39* was strong but not complete (**Table 1b**). However, the phenotype is clearly enhanced if individuals are also

heterozygous for the *ftz-fl* mutation. On the 14 *UAS-mGFP GAL4-201Y/UAS-Hr39; +/+* mushroom bodies, 71% (n = 10) show “strong” and 29% (n = 4) show “complete” phenotypes, respectively, while of the 12 *UAS-mGFP GAL4-201Y/UAS-Hr39; ftz-fl<sup>ex7</sup>/+* mushroom bodies analyzed, 17% (n = 2) show a “strong” phenotype and 83% (n = 10) a “complete” one ( $P < 0.01$  by  $\chi^2$  test). Mushroom bodies from *ftz-fl<sup>ex7</sup>/+* individuals displayed normal pruning (n = 20). We thus conclude that FTZ-F1 and HR39 may compete during the regulation of *EcR-B1* expression which underscores the importance of the observed repression of *Hr39* expression by FTZ-F1 during wild type axon pruning.

### ***Hr39* is required for normal $\alpha\beta$ neuron development**

The *GAL4-c739* GAL4 insertion within the *Hr39* gene strongly drives the expression of UAS-transgenes in adult-specific  $\alpha\beta$  mushroom body neurons<sup>23</sup>. This GAL4 enhancer trap may reflect, at least some aspects of, endogenous *Hr39* expression. However, we suspect the avidity of the anti-HR39 antibody is not sufficiently high enough to reliably detect the protein at the wild-type expression levels. Consequently, it was difficult to consistently see a significant difference in staining of wild type versus *Hr39* null mutant individuals.

Nevertheless, the *GAL4-c739* expression data indicates that *Hr39* is likely expressed in the mushroom body  $\alpha\beta$  neurons and may therefore have some role in their normal development. On the other hand, if *Hr39* over-expression induces a blockade of  $\gamma$  neuron remodeling then one would expect the gene to normally be down regulated in these neurons. Consequently, individuals bearing a null mutation of *Hr39* could show normal  $\gamma$  axon pruning but display  $\alpha\beta$  axon defects. As expected, this was indeed the case; 100% of the *Hr39<sup>-/-</sup>* mushroom bodies had wild-type  $\gamma$  axons and 60% (n = 50) had defects in  $\alpha\beta$  axons including  $\alpha\beta$  axon defasciculation and  $\alpha$  axon misguidance (**Fig. 6b** versus **6a** and also **Table 1f** for *Hr39<sup>-/-</sup>* neuroblast clones ).

Finally, we ascertained whether ectopic expression of FTZ-F1 in these neurons, which normally express *Hr39*, could down regulate *Hr39* expression as monitored by the use of *GAL4-c739* and *UAS-GFP*. Forced *ftz-f1* expression resulted in significantly decreased *Hr39* transcription as indicated by diminished GFP expression (**Fig. 6c–e** for quantification). Forced expression of *βftz-f1* in  $\alpha\beta$  neurons was not seen to alter cell fate specification (**Supplementary Fig. 13**). Thus, *Hr39* plays roles in  $\alpha\beta$  axon guidance and fasciculation but is, however, necessarily down regulated in  $\gamma$  axons for pruning to occur.

### ***in vivo* binding of FTZ-F1 on the *EcR* locus**

A 9-bp consensus binding sequence for FTZ-F1 (5'-YCAAGGYCR-3') is defined<sup>32,33</sup>. We have confirmed the *in vitro* binding of FTZ-F1 to this consensus sequence (**Supplementary Fig. 14**). Consequently, we scanned the 78 kb *EcR* locus for the 8 possible nucleotide combinations resulting from this consensus sequence on both strands. The location of these sites on the *EcR* locus is shown (**Fig. 7a**). We found 9 putative FTZ-F1 binding sites (**Fig. 7b**). Chromatin immunoprecipitation from L3 brains with anti-FTZ-F1 antibodies was performed and the 6 potential FTZ-F1-binding sites upstream of *EcR-B1* transcription start site were monitored. The results clearly established that the FTZ-F1 protein binds to a subset of the consensus sites in the presumptive *EcR-B1* gene promoter just prior to remodeling (**Fig. 7c**).

## **DISCUSSION**

### **Roles of *βftz-f1* and *Hr39* in neuronal remodeling**

Developmental axon pruning is a fundamental process underlying nervous system maturation. The developmental axon pruning of  $\gamma$  neuron in mushroom bodies is a paradigm for localized degeneration and shares some molecular and cellular features with axon degeneration after

nerve injury<sup>2</sup>. Seminal studies have revealed a cell-autonomous TGF- $\beta$  signaling pathway role in modulating the *EcR-B1/usp* ecdysone receptor during  $\gamma$  axon pruning<sup>3,4</sup>. During *Drosophila* metamorphosis several primary response genes, induced directly by the ecdysone/ECR/USP complex, have been identified. Many direct targets of this complex are nuclear-receptors. Particularly, three early regulatory genes: the *Broad-Complex*, *E74* and *E75* are primary targets of the ecdysone cascade<sup>15,34</sup>. Surprisingly, these primary targets are dispensable for mushroom body neuronal remodeling leading to the hypothesis that novel downstream genes are involved in regulating developmental axon pruning<sup>3</sup>. Nevertheless, a recent micro array study has shown that global ECR targets are also targets of ecdysone in mushroom body neurons despite the fact that most are not required for axon pruning<sup>10</sup>. We found that homologous nuclear receptors *ftz-f1* and *Hr39* play key roles in the pruning process. Neither *ftz-f1* nor *Hr39* are found to be ECR targets in the aforementioned global genomic analysis of neuronal remodeling. Our data clearly demonstrated a requirement for *ftz-f1* expression and a simultaneous silencing of *Hr39* in  $\gamma$  neurons for appropriate pruning to occur. To our knowledge a role for FTZ-F1 in nervous system development has not been yet described. Thus, our results demonstrating an essential role in  $\gamma$  neuron remodeling opens the door to new studies of FTZ-F1 function in the control of nervous system development.

Since *Hr39* has to be silenced (or at least kept to a low level of expression) in the  $\gamma$  neurons for the pruning to occur, the mechanism of its repression is of fundamental importance. The obvious candidates that may down-regulate *Hr39* in the  $\gamma$  neurons, TGF- $\beta$ /*babo* signaling and *EcR-B1* itself have likely been excluded by our studies here. Instead, our results showed that *Hr39* was down-regulated in the  $\gamma$  neurons by FTZ-F1.

Mushroom bodies are involved in olfactory and courtship conditioning memory<sup>35,36</sup>. How memory is affected in pruning deficient adult animals which display immature larval-stage neuronal circuitry may help unravel the functional role of neuron remodeling. Unlike

*EcR-B1*, *usp* or *ftz-fl* null mutants, *Hr39* over-expressors are viable as adults and will make it possible to ultimately assess the requirement for wild-type mushroom body pruning in memory by testing adults with  $\gamma$  pruning defects.

### **Regulation of *EcR-B1* expression by the *ftz-fl/Hr39* pathway**

The most surprising result of this study was finding that the *EcR-B1* gene is targeted by FTZ-F1/HR39 during  $\gamma$  neuron pruning and likely not *vice versa* as expected. Nuclear receptor genes, including *ftz-fl* and *Hr39* are transcriptionally-regulated by ecdysone and show mRNA changes in phase with ecdysone pulses during development<sup>15</sup>. Therefore, we predicted that the *ftz-fl* and *Hr39* genes, if involved in mushroom body neuron remodeling, would be targets of the ecdysone-ECR-B1-USP complex. Here we have shown that, contrary to expectations, *EcR-B1* is a genetic target and likely a direct target of *ftz-fl/Hr39* protein products. We have provided molecular evidence that FTZ-F1 binds *in vivo* and in the expected tissue the *EcR* locus at several consensus sites.

We propose that *ftz-fl* has two roles in  $\gamma$  axon pruning: (i) to participate directly in *EcR-B1* activation and (ii) to participate indirectly in *EcR-B1* activation by directly repressing *Hr39* activity. The repression of *Hr39* activity is crucial because the presence of HR39 protein in the  $\gamma$  neurons during pruning would block neuron remodeling by down-regulating *EcR-B1* activation, presumably by functionally competing with FTZ-F1. Nevertheless, HR39 alone, when FTZ-F1 is absent, is able to repress *EcR-B1* expression (**Supplementary Fig. 9j**).

### **Two pathways regulate *EcR-B1* in neuron remodeling**

As schematically depicted (**Supplementary Fig. 15**) two different pathways are involved during  $\gamma$  axon pruning. *EcR-B1* is specifically expressed in larval  $\gamma$  neurons<sup>3</sup>. As has

previously been described, TGF- $\beta$  signaling through the dActivin receptor activates *EcR-B1* although it is not known how cell type-specific responses are achieved <sup>4</sup>. A second, independent pathway acting in parallel with dActivin might provide such specificity. The *ftz-fl/Hr39* pathway may be such a pathway that provides *EcR-B1* activation specificity. Nevertheless, here again the mechanism of cell type-specificity is not obvious since *ftz-fl* seems to be expressed broadly, if not ubiquitously, in the second instar brain. A putative specific ligand or co-factor for FTZ-F1 may ensure such specificity.

Thus, *EcR-B1* is the point of convergence for at least two independent pathways that ensure its differential expression required for a specific neuron remodeling process. Understanding how these different signals are integrated to regulate *EcR-B1* to facilitate axon pruning, will be necessary step to unravel the molecular mechanisms underlying this fundamental process of nervous system maturation.

### **Acknowledgements**

We are particularly grateful to Lee Fradkin for helpful discussions and comments on the manuscript. We thank Liqun Luo and Tzumin Lee for *babo*, *usp* and several MARCM stocks, Hitoshi Ueda for the *ftz-fl<sup>ex7</sup>* *FRT2A* stock, the pUAST- $\beta$ *ftz-fl* vector and the anti-FTZ-F1 antibody, Craig Woodard for the *ftz-fl<sup>19</sup>* stock, Leslie Pick for the *UAS- $\alpha$ ftz-fl* stock and the GST-FTZ-F1 expression vector, Carl Thummel for the anti-ECR-B1 antibody (ascite fluid), Barry Dickson for the anti-TRIO antibody, Mike O'Connor for the *UAS-babo-act* (1B3-strong) and the *UAS-babo $\Delta$ I* (2 transgenes 5A2-8A2) stocks, and unpublished data pertaining to anti-BABO and to *babo* transcripts and Kathy Matthews and Kevin Cook at the Bloomington *Drosophila* Stock Center. We also thank Nicole Lautredou at the CRIC and Julien Cau at the "Plateau d'Imagerie Cellulaire" for help with confocal imaging and Patrick Atger and Cyril Sarrauste de Menthière at the "service iconographie IGH". Transgenic lines

were generated by BestGene, Inc. This work was supported by the CNRS, by grants from the Fondation pour la Recherche Médicale, the EEC Marie–Curie 5th framework, the Association pour la Recherche sur la Cancer (n° 3744), the Association Française contre les Myopathies (MNM1 2007) and the Agence Nationale de la Recherche (ANR–07–NEURO–034–01).

A.B. was supported by a postdoctoral fellowship from FRM, EEC Marie–Curie 5th framework, from AFM and from ANR. C.C.R. was supported by a joint PhD grant from the CNRS and Région Languedoc–Roussillon and then by a predoctoral ARC fellowship. A.B. and C.C.–R. contributed equally to this work.

### **Author contributions**

A.B., C.C.–R. and J.–M.D. designed the experiments and analyzed the data. C.F. and F.J. performed the ChIP experiments. J.–M.D. carried out the elaboration of the genetic stocks. A.B., C.C.–R., M.F., A.F., T.G. performed all the other experiments. The manuscript was written by J.–M.D. and commented by A.B., C.C.–R. and A.F.

**Table 1**

Genotype	N	Mutant pruning phenotype			
		WT	weak	strong	complete
a) <i>ftz-f1</i> mutant and rescue (neuroblast clones)					
<i>ftz-f1<sup>-/-</sup></i>	28	0	0	19	9
<i>ftz-f1<sup>-/-</sup> + UAS-βftz-f1</i> (II)	10	9	1	0	0
<i>ftz-f1<sup>-/-</sup> + UAS-βftz-f1</i> (III)	18	15	3	0	0
<i>ftz-f1<sup>-/-</sup> + UAS-αftz-f1</i>	11	10	1	0	0
<i>ftz-f1<sup>-/-</sup> + UAS-EcR-B1</i>	16	16	0	0	0
b) HR39 overexpression and rescue (brains)					
<i>Hr39<sup>C13</sup></i>	>10	0	0	>10	0
<i>Hr39<sup>C13</sup> + UAS-lacZ</i>	18	0	0	18	0
<i>Hr39<sup>C13</sup> + UAS-EcR-B1</i>	44	44	0	0	0
<i>UAS-Hr39</i>	44	0	0	40	4
<i>UAS-Hr39 + UAS-EcR-B1</i>	22	22	0	0	0
c) FTZ-F1 and HR39 competition (neuroblast clones)					
<i>Hr39<sup>C13</sup></i>	10	0	0	3	7
<i>Hr39<sup>C13</sup> + UAS-βftz-f1</i> (II)	16	2	14	0	0
<i>UAS-Hr39</i>	26	0	0	0	26
<i>UAS-Hr39 + UAS-βftz-f1</i> (II)	27	7	20	0	0
d) <i>babo</i> mutant and rescue (neuroblast clones)					
<i>babo<sup>-/-</sup></i>	>10	0	0	0	>10
<i>babo<sup>-/-</sup> + UAS-EcR-B1</i>	13	0	0	10	3
<i>babo<sup>-/-</sup> + Hr39<sup>-/-</sup></i>	9	0	0	0	9
<i>babo<sup>-/-</sup> + Hr39<sup>-/-</sup> + UAS-EcR-B1</i>	19	0	0	15	4
<i>babo<sup>-/-</sup> + Hr39<sup>-/-</sup> + UAS-βftz-f1</i> (III)	19	0	0	0	19
<i>babo<sup>-/-</sup> + UAS-βftz-f1</i> (III)	9	0	0	0	9
<i>UAS-βftz-f1</i> (II)	15	15	0	0	0
e) <i>usp</i> mutant and rescue (neuroblast clones)					
<i>usp<sup>-/-</sup></i>	>10	0	0	0	>10
<i>usp<sup>-/-</sup> + Hr39<sup>-/-</sup></i>	16	0	0	0	16
<i>usp<sup>-/-</sup> + UAS-αftz-f1</i> (II)	11	0	0	0	11
<i>usp<sup>-/-</sup> + Hr39<sup>-/-</sup> + UAS-βftz-f1</i> (II)	10	0	0	0	10
f) <i>ftz-f1</i> mutant rescued by <i>Hr39</i> null (neuroblast clones)					
<i>Hr39<sup>-/-</sup></i>	10	10	0	0	0
<i>ftz-f1<sup>-/-</sup></i>	28	0	0	19	9
<i>ftz-f1<sup>-/-</sup> + Hr39<sup>-/-</sup></i>	37	0	14	23	0

## Figure and Table legends

**Figure 1**  $\beta$ FTZ–F1 is required for  $\gamma$  neuron Pruning. Expression of *GAL4–201Y* driven GFP (green) and FASII (red) in adult  $\gamma$  neurons. **(a, b)** Mature axons of wild–type MARCM clones. **(d, e)** Pruning deficits in *ftz–f1<sup>-/-</sup>* mutant MARCM clones. **(a)** A wild type neuroblast clone where GFP expression is observed in three axon bundles: the large dense lobe of adult  $\gamma$  neurons (arrow) and the weak  $\alpha$  and  $\beta$  core bundles (arrowheads). **(b)** Wild type single–cell clone. Arrowhead points to the cell body. Note the presence of only a single medial branch. **(c)** Forced expression of  $\beta$ FTZ–F1 does not affect  $\gamma$  neuron pruning. **(d)** The absence of FTZ–F1 blocks  $\gamma$  neuron pruning. Arrows point to the larval–type  $\gamma$  neurons surrounding the dorsal and medial  $\alpha\beta$  lobes defined by the FASII labeling. The asterisk indicates the area where remodeled  $\gamma$  neuron axons should be located. **(e)** Two cell clones of *ftz–f1<sup>-/-</sup>* mutant. Arrowheads label the cell bodies. Note the presence of two dorsal (arrow) and medial branches. **(f)** Forced expression of  $\beta$ FTZ–F1 in  $\gamma$  neurons completely rescues the *ftz–f1<sup>-/-</sup>* pruning mutant phenotype. Scale bar is 20  $\mu$ m. All these pictures are composite confocal images except for **b** and **e** which are deconvoluted Z–stacks. See genotypes in **Supplementary list of fly strains**.

**Figure 2** HR39 ectopic expression blocks  $\gamma$  neuron remodeling. **(a–c)** Wild type adult brain, wild type neuroblast and wild type single–cell clone respectively, labeled with GFP under the control of *GAL4–201Y* in which all the  $\gamma$  neurons have been remodeled. **(d–f)** Lack of larval pruning, in most of the  $\gamma$  neurons, caused by ectopic expression of HR39 respectively in a brain, a neuroblast and a double two–cell clone. Arrows label un–pruned  $\gamma$  neurons. An asterisk labels remodeled  $\gamma$  neurons. Un–pruned  $\gamma$  neurons show higher GFP intensity than the remodeled one, likely due to GFP accumulation in these neurons because of the persistence of

these axons all along development. Note in **f** the presence of two un-pruned  $\gamma$  axons and two apparently pruned  $\gamma$  axons. Scale bar is 20  $\mu\text{m}$ . See genotypes in **Supplementary list of fly strains**. **(g)** Molecular map of the *Hr39* locus with the intron/exon structure of the two main categories of mRNAs. The positions of the *P* element insertions in *Hr39*<sup>C13</sup> and *Hr39*<sup>GS9939</sup> are shown by a triangle. The *Hr39*<sup>C105</sup> remaining regions after imprecise excision of the *P*[*GSV6*] element are indicated by lines. **(h)** Expression of HR39 detected by Western blot of adult heads. Two lanes of control (+/+) and two lanes of mutant (*Hr39*<sup>C105</sup>/*Df*(2L)*Exel6048*) samples were loaded. The two bands at 87 and 74 KDa, corresponding respectively to the long and the short HR39 proteins, are absent in mutant samples. Un-cropped full-length blots are presented in **Supplementary Fig. 16**.

**Figure 3** Forced expression of ECR-B1 rescues *ftz-f1*<sup>-/-</sup> and HR39 over-expression  $\gamma$  neuronal remodeling defects. **(a)** Pruning/remodeling defects observed in *ftz-f1*<sup>-/-</sup> mutant neuroblast clones are rescued **(c)** by forced ECR-B1 expression. **(b)** HR39 over-expression phenotype is also rescued **(d)** by ECR-B1. Green represents *GAL4-201Y*-driven GFP and red is anti-FASII. All panels are composite confocal images. The scale bar is 20  $\mu\text{m}$ . Genotypes: **(a)** *hs-FLP/X; UAS-mCD8GFP GAL4-201Y/+; ftz-f1*<sup>ex7</sup> *FRT2A/tubP-GAL80 FRT2A* **(c)** *hs-FLP/X; UAS-mCD8GFP GAL4-201Y/+; ftz-f1*<sup>ex7</sup> *FRT2A UAS-EcR-B1/tubP-GAL80 FRT2A* **(b)** *UAS-Hr39 /UAS-mCD8GFP GAL4-201Y* **(d)** *UAS-Hr39/UAS-mCD8GFP GAL4-201Y; UAS-EcR-B1/+*. See full genotypes in **Supplementary list of fly strains**.

**Figure 4** Expression of ECR-B1 depends on normal FTZ-F1 and lack of HR39 activity in  $\gamma$  neurons. Composite confocal images of the mushroom body cell body regions in late third instar larval brains are shown. Green represents *GAL4-201Y*-driven GFP and red is anti-ECR-B1. **(a, b)** Brains containing wild type and **(c, d)** *ftz-f1*<sup>-/-</sup> mutant MARCM clones were

immunostained for ECR–B1 expression. The white outline indicates the extent of GFP labeling of the cell bodies belonging to the clone. **(f, g)** Brains containing wild type and **(h, i)** HR39–overexpressing  $\gamma$  neurons were immunostained for ECR–B1 expression. The white outline reveals the extent of GFP labeling contained in the cell body of the  $\gamma$  neurons of the brain. **(b)** Some GFP labeling not enclosed by the outline likely corresponds to neurites. Note that ECR–B1 is present in the nuclei of  $\gamma$  neurons in wild type neuroblast clones and brains **(b, g)**. However, ECR–B1 could barely be detected either in the *ftz–fI<sup>ex7</sup>* mutant neuroblast clones or in the HR39–overexpressing  $\gamma$  neurons **(d, i)**. **(e, j)** Anti–ECR–B1 signal quantifications in arbitrary units. Results are means and SEM. In **(e)**,  $n = 22$  for wild type and 23 for mutant. In **(j)**,  $n = 48$  for wild type and 47 for mutant. The differences are highly significant in a *t*–test (both two–tailed *P* values are  $< 0.0001$ ). Scale bars are 10  $\mu\text{m}$ . See genotypes in **Supplementary list of fly strains**.

**Figure 5** FTZ–F1 represses *Hr39* expression in order to prevent competition.

**(a–c)** Un–pruned  $\gamma$  axons phenotypes. Un–pruned  $\gamma$  axons are indicated by arrows and pruned  $\gamma$  axons are pointed by an asterisk in **a** and **b**. In **c** the arrowhead point to wild type  $\gamma$  neuron that do not belong to the clone. **(a)** “Weak” phenotype, **(b)** “strong” phenotype and **(c)** “complete” phenotype. Green represents *GAL4–201Y* driven GFP and red is anti–FASII. Scale bar is 20  $\mu\text{m}$ .

**(d–i)** *Hr39* is repressed by FTZ–F1 in  $\gamma$  neurons. **(d–f)** Brains containing *GAL4–201Y* driven GFP labeled MARCM control clones and **(g–i)** *ftz–fI<sup>-/-</sup>* mutant clones (green) were immunostained for HR39 expression (red). HR39 is over–expressed (1.78x) in *ftz–fI<sup>-/-</sup>* clones when compared to wild–type clones. Results are means and SEM. The differences are significant in a *t*–test (the two–tailed *P* value is  $< 0.001$ ). Scale bar is 20  $\mu\text{m}$ .

(j-l) *in vivo* competition between HR39 and  $\beta$ FTZ-F1 for  $\gamma$  Neuron Remodeling. (j) MARCM neuroblast clones over-expressing HR39 were (k) partially or (l) completely rescued by  $\beta$ FTZ-F1. Arrow in k indicates some un-pruned  $\gamma$  neurons. Titration of GAL4 can be ruled out as having an effect here since the addition of an *UAS-lacZ* transgene does not change the *Hr39* over-expression phenotype (Table 1b). Pictures are composite confocal images. Green represents *GAL4-201Y* driven GFP and red represents anti-FASII. Scale bar is 20  $\mu$ m. See genotypes in **Supplementary list of fly strains**.

**Figure 6** *Hr39* is required for normal  $\alpha\beta$  neuron development but not for  $\gamma$  pruning. (a) Wild-type mushroom body. (b) *Hr39*<sup>-/-</sup> mushroom body where the  $\gamma$  axons appear wild-type ( $\gamma$ ) but  $\alpha$  axon misguidance is clearly apparent ( $\alpha$ ). Some axons from the  $\beta$  lobes ( $\beta$ ) show midline crossing defects (MC). Green represents *GAL4-201Y*-driven GFP and red is anti-FASII. (c) Wild-type neuroblast clone including  $\alpha\beta$  neurons reflecting *Hr39* expression. (d) *Hr39* expression is reduced as reflected by the decrease in *GAL4-c739*-driven GFP expression when FTZ-F1 expression is forced. (e) Quantifications of the GFP signal in arbitrary units. Results are means and SEM with  $n = 8$  in each case. The difference is highly significant in a *t*-test (the two-tailed *P* value is  $< 0.001$ ). When the same experiment is done with *UAS-lacZ* instead of *UAS- $\beta$ ftz-f1* no difference in GFP intensity is detected ( $11.1 \pm 0.4$ ,  $n = 8$  versus  $11.4 \pm 0.3$ ,  $n = 8$ , the two-tailed *P* value is  $> 0.5$ ) ruling out the possibility of GAL4 titration by an extra UAS sequence. (a-d) Are composite confocal images. Scale bars are 20  $\mu$ m. Genotypes: (a) *UAS-mCD8GFP GAL4-201Y/+*. (b) *Df(2L)Exel6048 UAS-mCD8GFP GAL4-201Y /Hr39<sup>C105</sup>*. (c) *hs-FLP tubP-GAL80 FRT19A/FRT19A; GAL4-c739 UAS-mCD8GFP/+*. (d) *hs-FLP tubP-GAL80 FRT19A/FRT19A; GAL4-c739 UAS-mCD8GFP/UAS- $\beta$ ftz-f1*. See full genotypes in **Supplementary list of fly strains**.

**Figure 7** *in vivo* binding of FTZ–F1 upstream of the *EcR–B1* transcription start site. (a) Location of FTZ–F1 putative binding sites on the *EcR* locus is pointed by a corresponding triangle on both strands. (b) 9 putative FTZ–F1 binding sites are present. (c) Chromatin Immuno–Precipitation from L3 brains with anti–FTZ–F1 antibodies was performed for the 6 sites that are upstream of *EcR–B1* transcription start site. FTZ–F1 binds more on the A, B, C and D sites than on a control site in the RP49 locus. The differences are highly significant in a *t*–test (the two–tailed *P* value is either = 0.001 (\*\*)) or < 0.001 (\*\*\*)). The two last sites (E and F) do not show a significant retention of the FTZ–F1 protein when compared to the control RP49 site.

**Table 1**  $\gamma$  Neuron phenotypes obtained for each type of experiment. Genotypes are indicated on the left. N indicates the number of mushroom body or mushroom body neuroblast clones observed for each genotype. The  $\gamma$  neuron phenotype was ranked into four categories: “WT” indicates a wild type pruning in which all the  $\gamma$  neurons are remodeled, “weak”, “strong” and “complete” refer to different level of mutant pruning phenotype (see **Fig. 5a–c** and “Range of mutant pruning phenotype” in Methods). *P* < 0.001 when *ftz–f1<sup>-/-</sup>* and *ftz–f1<sup>-/-</sup> + Hr39<sup>-/-</sup>* are compared with a  $\chi^2$  test. The *UAS* constructs are under the control of the *GAL4–201Y* driver.

## METHODS

***Drosophila* stocks.** All strains were maintained on standard culture medium at 25 °C. Except where otherwise stated, alleles have been described previously (<http://flystocks.bio.indiana.edu>).

**Molecular characterization of GAL4 enhancer trap strain *c739*.** BDGP inverse PCR protocol (<http://www.fruitfly.org/about/methods/inverse.pcr.html>) was used to localize the

*P{GawB}* transposon in the *c739* strain. The primer set *Pry1* (5'–CCTTAGCATGTCCGTGGGGTTTGAAT–3') and *Pry4* (5'–CAATCATATCGCTGTCTCACTCA–3') was used to amplify the sequence flanking the *P* 3' end. Two independent PCR products were sequenced with the *Pry2* (5'–CTTGCCGACGGGACCACCTTATGTTATT–3') primer. In the *c739* strain, the *P*–element is located in the second intron of *Hr39* (39B4 cytogenetic region) approximately 9.5 kb upstream of the ATG start codon.

***P*–element replacement.** The general method of *P* replacement is described<sup>37</sup>. 240 dysgenic males *P{Mae–UAS.6.11}* *y*<sup>+</sup>; *P{GawB}* *w*<sup>+</sup>/+; *Sb Δ2.3* /+ were produced by standard genetic crosses. The features and utilization of *P{Mae–UAS.6.11}* have been described<sup>38</sup>. The *Δ2–3* chromosome bears a stable integrated source of transposase<sup>39</sup>. These males were individually crossed with *y w*<sup>67c23</sup> females. We screened the progeny of each cross for *P* replacement by the absence of *w*<sup>+</sup> and the presence of *y*<sup>+</sup>. 30 potential *P* replacements were isolated. We screened 9 precise replacements of *P{GawB}* by *P{Mae–UAS.6.11}* using genomic PCR with two different primer sets. Primer set #1 combined primers *5'c739* (5'–CGCGACAAAGAGCATCTAA–3') and *OUY 52* (ACACAACCTTTCCTCTCAACAA: BDGP protocol), annealing at 1 kb upstream of the *P{GawB}* insertion site and in the 5' end of the *P* element, respectively; primer set #2 combined primers *3'c739* (5'–GCTAGGGCTCCTTTTCATA–3') and *OUY 52*, annealing at 1 kb downstream of the *P{GawB}* primer and in the 5' end of the *P* element, respectively. Using these two primer sets, we determined that in three *P* replacements the 5' end of the *P{Mae–UAS.6.11}* situate the UAS sequences in the correct orientation to drive expression. Finally, a Southern blot using an UAS–specific probe was performed to confirm these results. We used the *P{Mae–UAS.6.11}–Hr39<sup>C13</sup>* *P* replacement to over–express *Hr39*<sup>+</sup> called here in short *Hr39<sup>C13</sup>*.

**P-element imprecise excision and production of the *Hr39* null mutation.** Individuals simultaneously carrying a *P* element in the *Hr39* gene and a deficiency removing the entire *Hr39* locus together with the transposase source were generated. This was done in order to prevent imprecise excisions being repaired from the wild-type homologous chromosome<sup>40</sup>. Thus, *y w<sup>67c23</sup>; P{GS9939-UAS}-HR39/ Sp Df(2L)Exel6048; Sb Δ2.3* /+ dysgenic males were crossed with *y w<sup>67c23</sup>; CyO/Sp* females and male progeny of the genotype *y w<sup>67c23</sup>; Hr39<sup>Pexcw-</sup>/CyO; +/+ [w<sup>-</sup>, Sp<sup>+</sup> and Sb<sup>+</sup>]* were screened. 250 excision lines were established from independent events and screened by PCR for loss of the ATG codon. The *Hr39<sup>C105</sup>* line is viable in homozygous conditions and shows an excision of around 8 kb of genomic DNA starting 7.4 kb upstream of the ATG and removing 520 bp of the coding sequence (see **Fig. 2g**).

**Dissection of brains, visualization of mushroom bodies and MARCM mosaic analysis.**

Larval, pupal and adult brains were dissected and treated as previously described<sup>38</sup>. For the clonal analysis study (MARCM) the clones were induced in first instar by applying a 1 h heat-shock at 37 °C as previously described<sup>12, 24</sup>. The anti-FASII (1D4) was obtained from the Developmental Studies Hybridoma Bank and used at 1:10. Mouse primary antibody against ECR-B1 (AD4.4)<sup>41</sup> was used at 1:5,000. Secondary antibody goat anti-mouse conjugated to Cy3 (Jackson) was used at 1:300.

**Range of mutant pruning phenotype.** A phenotype was considered to be “weak” (**Fig. 5a**) when few un-pruned individual axons were observed in the dorsal lobe. A phenotype was considered as “strong” (**Fig. 5b**) when > 50% of the axons are un-pruned. These un-pruned axons are often organized in thick bundle along the dorsal lobe. A mix of pruned and un-pruned axons was observed in the medial lobe where un-pruned axons are located out of the

plan of the normally pruned adult  $\gamma$  axons and also display high GFP expression. The percentage of un-pruned axons is estimated by the width of the corresponding medial bundle compared with the width of the medial pruned axon bundle, requiring visualization of the same clone at several different focal planes. The “complete” mutant phenotype does not contain any visible pruned axons (**Fig. 5c**).

**FTZ-F1 and HR39 antibody staining.** The rabbit primary antibodies against FTZ-F1<sup>26</sup> and HR39 antibody were preabsorbed with 20 *yw<sup>c</sup>* and *Hr39<sup>-/-</sup>* heads and thoraces, respectively (300  $\mu$ l of antibody in PBS Triton 3% at the final dilution 1:10,000). After larval or adult brain dissection and fixation in 3,7% formaldehyde, washes and antibody incubations were all done in PBS with 3% Triton-X100 and 5% BSA. Before primary antibody incubation, brains were saturated in 5% BSA for 48 h, antibodies were subsequently applied for 5 h and then the brains washed for 12 h. Cy3-conjugated Goat anti-rabbit (Jackson Laboratories) and Alexa 568-conjugated goat anti-guinea pig (Molecular Probes) were employed as secondary antibodies for 2 h followed by wash steps, mounting and visualization.

**Microscopy and image processing.** Images were taken either by a confocal microscope (Bio-Rad MRC 1024 or a Leica SP2 UV) or by a fluorescence microscope (Leica DM 6000). In the latter case, a 3D-deconvolution step was performed (Huygens deconvolution software). Contrasts and relative intensities of the green (GFP) and red (Cy3 – Alexa 568) were adjusted with Photoshop (Adobe) and ImageJ.

**Quantification of immunolabelling.** For quantification, cell contours were drawn from GFP channel using Photoshop software. This allowed us to quantify intensities using ImageJ software from CY3 channel. We performed measurements in GFP positive cells (Intensity

1,..., n) and the same number of measurements in background. The mean of these background measurements is called mean-background. We then subtracted intensities of mean-background from each intensity value (Intensity 1,..., n – mean-background) to obtain real intensity values. Finally, we compared real intensity values of the 2 genetic conditions using a statistical *t* test. In the case of measuring the effect of lack of *ftz-fl* function on HR39 expression (**Fig. 5d-i**), 10 animals were compared since, in total, we assayed 5 clones for controls and 5 clones for experiments that were scored blindly and this was the result of three independent stains. We have measured groups of about 10 non-overlapping cells. N = 44 groups amongst the 5 control clones and N = 42 groups amongst the 5 mutant clones. We have then compared the values of the two genetic conditions using a statistical *t* test. The HR39 antibody is validated to measure over-expression (**Supplementary Fig. 12**). In the **Supplementary Figure 8** we have quantified in a similar way both the HR39 and the FTZ-F1 expression levels.

**Antibody production and Western analysis.** A 565 bp BamH1-Xho1 fragment encoding the HR39 N-terminal peptide was PCR-amplified from a pBluescript *Hr39* cDNA clone (see below) and inserted into pGEX-5X-1 (Amersham Pharmacia Biotech) in frame with the coding region for a GST tag, resulting in a fusion protein carrying 182 amino acids of HR39 corresponding to aa 5 through to aa 187. This part of the protein is not homologous to others *Drosophila* nuclear receptors. Purified GST-HR39 protein was injected into two guinea pigs (Eurogentec) and antisera were tested by Western blotting. Five *Drosophila* adult heads were homogenized in an Eppendorf tube containing 20 ul of 3X sample buffer (2% SDS, 0.125 M Tris-HCl pH 6.9, 5% β-mercaptoethanol, 20% glycerol, bromophenol blue) and proteins were separated by SDS-PAGE. After electrotransfer to nitrocellulose, the blot was blocked in PBS, 0.5% Tween-20, 5% milk. The *Drosophila* HR39 protein was detected using the

antibody at a dilution of 1:1,000 in PBS, 0.5% Tween-20, 5% milk and revealed using anti-guinea pig Ig horseradish peroxidase (1:3,000) and an ECL kit (Amersham). Before use the anti-HR39 antibody was preabsorbed with *Hr39*<sup>-/-</sup> third instar larvae.

**Construction of *UAS-Hr39* and *UAS-βftz-fl*.** A 3.3 kb SmaI-XhoI *Hr39* cDNA fragment was excised from the pOT2 vector (clone LD450 B9 from BDGP corresponding to the long protein) and cloned into the pBluescript KS(+) vector. Then a BglII-XhoI fragment was swapped into the pUAST transformation vector. A 2.5 kb EcoRI fragment containing the *βftz-fl* coding region was inserted into pUAST. P element transformation was performed by BestGene.

**Binding sites research.** The complete *EcR* locus (78.3 kb) was scanned for FTZ-F1 binding sites using the Biological sequence alignment editor (BioEdit) program (Ibis Biosciences).

**Chromatin immunoprecipitation followed by quantitative PCR analysis.** Third instar larval brains were dissected in PBS and kept on ice. Brains were pelleted by centrifugation at 4,000 g for 5 min, and fixed in buffer A (50 mM Hepes, 1 mM EDTA, 0.5 mM EGTA, 15 mM NaCl, 60 mM KCl, 0.1% tritonX-100 and Protease inhibitor cocktail SetI (Calbiochem)) containing 1.8% formaldehyde. After 12 min fixation, glycine was added to 0.225 M to stop crosslinking. Brains were washed in buffer A, resuspended in buffer B (50 mM Hepes, 1 mM EDTA, 1% NP40, 0.1% SDS, 0.1% NaDeoxycholate and Protease inhibitor cocktail SetI (Calbiochem)) containing 140 mM NaCl and disrupted with a pestle. Extract was sonicated 2 times 30 s on ice using the Vibra-Cell ultrasonic processor at amplitude 50, and 10 min (settings 30 s on, 30 s off, high power) using a Bioruptor (Diagenode). Debris were pelleted by centrifugation 5 min at 16,000 g. Soluble chromatin was pre-cleared 1 h with magnetic

protein-G Dynabeads (Invitrogen) at 4 °C. For immunoprecipitations, chromatin corresponding to approximately 25 brains was incubated overnight at 4 °C with a mixture of anti-FTZ-F1 antibodies (20  $\mu$ l of dC-16 from Santa Cruz Biotechnology + 0.5  $\mu$ l from <sup>26</sup>) or no antibody (Mock) in the presence of 30  $\mu$ l protein-G Dynabeads. Beads were washed at room temperature in buffer B containing 140 mM NaCl (3 x 5 min), then 300 mM NaCl (3 x 5 min), then 250 mM LiCl (2 x 5 min), and finally in TE (2 x 5 min). Elution from the beads was performed at 65 °C with 300  $\mu$ l elution buffer (100 mM NaHCO<sub>3</sub>, 1% SDS) and shaking. To reverse the crosslinks, NaCl was added to 300 mM and the tubes incubated 7 h at 65 °C. After RNase A and proteinase K treatments, we purified DNA by phenol-chloroform extraction and ethanol precipitation. The resulting DNA was dissolved in 60  $\mu$ l H<sub>2</sub>O.

Real-time PCR was performed using SYBR Green and the LightCycler 480 real-time PCR system (ROCHE), in 10  $\mu$ l with 2.5  $\mu$ l purified DNA per reactions. PCR settings: 2 min 95 °C; 45 cycles: 10 s 95 °C, 15 s 68 °C, 25 s 72 °C. PCR were performed in triplicates from at least 4 independent immunoprecipitations. For each PCR couple and each chromatin preparation, a standard curve was made on purified input DNA (aliquots of chromatin that did not undergo immunoprecipitation). The amount of target sequence in immunoprecipitated DNA samples was expressed as a percentage of DNA present in the input material. A fragment from the *Rp49* gene is used as a negative control.

Primers used:

A-Fwd: AGTCGAGAACGTGCCTTTCACCT

A-Rev: GGCTGGGTGTCCTGGGGGTT

B-Fwd: GACCGAAGGCTCGGCTCTGC

B-Rev: TTCGCTTCCTCGGCCCTCCC

C-Fwd: GCTGCTACTGCGGTGCCAGTT

C–Rev: TGTGCGACTCGCCAAAAGCCA  
D–Fwd: CATGCGGTGGGCGGTGGAAG  
D–Rev: AGCGGCTGGGGCGTAGAAGT  
E–Fwd: AGTAACGTGGAGCCTTGGGCA  
E–Rev: CCAGTGCGAGGGTGTGCGAA  
F–Fwd: CCCGGAAGCTCCTTTCTCGCC  
F–Rev: TCGCGCGCAATATTATTTCCATTCAA  
Rp49–Fwd: CACCAAGCACTTCATCCGCC  
Rp49–Rev: TTCTTGGAGGAGACGCCGTGG

**Real–time quantitative RT–PCR.** Total RNA from third larval instar brains was extracted using TRIZOL Reagent (Invitrogen) (40 brains for 40  $\mu$ l of TRIZOL) following the manufacturers’s instructions. For all the reverse transcription reactions, 1  $\mu$ g of total RNA was used. First–strand complementary DNA (cDNA) was synthesized with random hexamers as primers using the SuperScript first–strand synthesis system according to the manufacturer’s protocol (Invitrogen). An equal volume mixture of the products was used as the template for PCR amplification. The primers for *babo<sub>a</sub>* were ATGGGAGCATCATCTTCAGC (forward) and GAACCTTTCGTTACTGGTGAGG (reverse) (fragment length, 95 bp). The primers for RpL32 were CGACGCACTCTGTTGTCG (forward) and CTTCATCCGCCACCAGTC (reverse) (fragment length, 84 bp). Reactions were performed in a 20– $\mu$ l volume with 2  $\mu$ M each of forward and reverse primers, and Quantitect™ SYBR Green PCR Master Mix (Qiagen), using a LightCycler 480 instrument and software from Roche. Each sample was run in triplicate. PCR conditions included an initial denaturation step of 5 min at 95 °C followed by 45 cycles of PCR consisting of 10 s at 95 °C, 15 s at 58 °C, and 15 s at 72 °C. Cp values

from the triplicate PCR reactions for *babo<sub>a</sub>* were normalized against the average Cp values for RpL32 from the same cDNA sample.

**Statistics.** Comparison of two groups expressing a quantitative variable were analyzed for statistical significance using two-tailed Student's *t*-test and all error bars are expressed as  $\pm$  standard error of the mean (SEM). Comparison between groups expressing a qualitative variable were analyzed using the  $\chi^2$  test. Values of  $P < 0.05$  were considered significant.

## References

1. Williams, D.W. & Truman, J.W. Remodeling dendrites during insect metamorphosis. *J Neurobiol* 64, 24-33 (2005).
2. Luo, L. & O'Leary, D.D. Axon retraction and degeneration in development and disease. *Annu Rev Neurosci* 28, 127-156 (2005).
3. Lee, T., Marticke, S., Sung, C., Robinow, S. & Luo, L. Cell-autonomous requirement of the USP/EcR-B ecdysone receptor for mushroom body neuronal remodeling in *Drosophila*. *Neuron* 28, 807-818 (2000).
4. Zheng, X., *et al.* TGF-beta signaling activates steroid hormone receptor expression during neuronal remodeling in the *Drosophila* brain. *Cell* 112, 303-315 (2003).
5. Watts, R.J., Hoopfer, E.D. & Luo, L. Axon pruning during *Drosophila* metamorphosis: evidence for local degeneration and requirement of the ubiquitin-proteasome system. *Neuron* 38, 871-885 (2003).
6. Awasaki, T., *et al.* The *Drosophila* trio plays an essential role in patterning of axons by regulating their directional extension. *Neuron* 26, 119-131 (2000).
7. Watts, R.J., Schuldiner, O., Perrino, J., Larsen, C. & Luo, L. Glia engulf degenerating axons during developmental axon pruning. *Curr Biol* 14, 678-684 (2004).
8. Awasaki, T., *et al.* Essential role of the apoptotic cell engulfment genes *draper* and *ced-6* in programmed axon pruning during *Drosophila* metamorphosis. *Neuron* 50, 855-867 (2006).
9. Schuldiner, O., *et al.* piggyBac-based mosaic screen identifies a postmitotic function for cohesin in regulating developmental axon pruning. *Dev Cell* 14, 227-238 (2008).
10. Hoopfer, E.D., Penton, A., Watts, R.J. & Luo, L. Genomic analysis of *Drosophila* neuronal remodeling: a role for the RNA-binding protein *Boule* as a negative regulator of axon pruning. *J Neurosci* 28, 6092-6103 (2008).
11. Ito, K., Awano, W., Suzuki, K., Hiromi, Y. & Yamamoto, D. The *Drosophila* mushroom body is a quadruple structure of clonal units each of which contains a virtually identical set of neurones and glial cells. *Development* 124, 761-771 (1997).
12. Lee, T., Lee, A. & Luo, L. Development of the *Drosophila* mushroom bodies: sequential generation of three distinct types of neurons from a neuroblast. *Development* 126, 4065-4076 (1999).
13. Williams, D.W. & Truman, J.W. Cellular mechanisms of dendrite pruning in *Drosophila*: insights from in vivo time-lapse of remodeling dendritic arborizing sensory neurons. *Development* 132, 3631-3642 (2005).

14. Brown, H.L., Cherbas, L., Cherbas, P. & Truman, J.W. Use of time-lapse imaging and dominant negative receptors to dissect the steroid receptor control of neuronal remodeling in *Drosophila*. *Development* 133, 275-285 (2006).
15. King-Jones, K. & Thummel, C.S. Nuclear receptors--a perspective from *Drosophila*. *Nat Rev Genet* 6, 311-323 (2005).
16. Horner, M.A., Chen, T. & Thummel, C.S. Ecdysteroid regulation and DNA binding properties of *Drosophila* nuclear hormone receptor superfamily members. *Dev Biol* 168, 490-502 (1995).
17. Yamada, M., *et al.* Temporally restricted expression of transcription factor betaFTZ-F1: significance for embryogenesis, molting and metamorphosis in *Drosophila melanogaster*. *Development* 127, 5083-5092 (2000).
18. Sullivan, A.A. & Thummel, C.S. Temporal profiles of nuclear receptor gene expression reveal coordinate transcriptional responses during *Drosophila* development. *Mol Endocrinol* 17, 2125-2137 (2003).
19. Ayer, S., *et al.* Activation and repression of *Drosophila* alcohol dehydrogenase distal transcription by two steroid hormone receptor superfamily members binding to a common response element. *Nucleic Acids Res* 21, 1619-1627 (1993).
20. Ohno, C.K., Ueda, H. & Petkovich, M. The *Drosophila* nuclear receptors FTZ-F1 alpha and FTZ-F1 beta compete as monomers for binding to a site in the fushi tarazu gene. *Mol Cell Biol* 14, 3166-3175 (1994).
21. Crispi, S., Giordano, E., D'Avino, P.P. & Furia, M. Cross-talking among *Drosophila* nuclear receptors at the promiscuous response element of the ng-1 and ng-2 intermolt genes. *J Mol Biol* 275, 561-574 (1998).
22. Guichet, A., *et al.* The nuclear receptor homologue Ftz-F1 and the homeodomain protein Ftz are mutually dependent cofactors. *Nature* 385, 548-552 (1997).
23. Yang, M.Y., Armstrong, J.D., Vilinsky, I., Strausfeld, N.J. & Kaiser, K. Subdivision of the *Drosophila* mushroom bodies by enhancer-trap expression patterns. *Neuron* 15, 45-54 (1995).
24. Lee, T. & Luo, L. Mosaic analysis with a repressible cell marker for studies of gene function in neuronal morphogenesis. *Neuron* 22, 451-461 (1999).
25. Wang, J., Zugates, C.T., Liang, I.H., Lee, C.H. & Lee, T. *Drosophila* Dscam is required for divergent segregation of sister branches and suppresses ectopic bifurcation of axons. *Neuron* 33, 559-571 (2002).
26. Murata, T., Kageyama, Y., Hirose, S. & Ueda, H. Regulation of the EDG84A gene by FTZ-F1 during metamorphosis in *Drosophila melanogaster*. *Mol Cell Biol* 16, 6509-6515 (1996).
27. Bellen, H.J., *et al.* The BDGP gene disruption project: single transposon insertions associated with 40% of *Drosophila* genes. *Genetics* 167, 761-781 (2004).
28. Horner, M. & Thummel, C.S. Mutations in the DHR39 orphan receptor gene have no effect on viability. *Dros. Info. Serv.* 80, 35-37 (1997).
29. Allen, A.K. & Spradling, A.C. The Sf1-related nuclear hormone receptor Hr39 regulates *Drosophila* female reproductive tract development and function. *Development* 135, 311-321 (2008).
30. Lavorgna, G., Karim, F.D., Thummel, C.S. & Wu, C. Potential role for a FTZ-F1 steroid receptor superfamily member in the control of *Drosophila* metamorphosis. *Proc Natl Acad Sci U S A* 90, 3004-3008 (1993).
31. Lam, G. & Thummel, C.S. Inducible expression of double-stranded RNA directs specific genetic interference in *Drosophila*. *Curr Biol* 10, 957-963 (2000).
32. Ueda, H., Sonoda, S., Brown, J.L., Scott, M.P. & Wu, C. A sequence-specific DNA-binding protein that activates fushi tarazu segmentation gene expression. *Genes Dev* 4, 624-635 (1990).
33. Ueda, H. & Hirose, S. Defining the sequence recognized with BmFTZ-F1, a sequence specific DNA binding factor in the silkworm, *Bombyx mori*, as revealed by direct sequencing of bound oligonucleotides and gel mobility shift competition analysis. *Nucleic Acids Res* 19, 3689-3693 (1991).
34. Thummel, C.S. Molecular mechanisms of developmental timing in *C. elegans* and *Drosophila*. *Dev Cell* 1, 453-465 (2001).

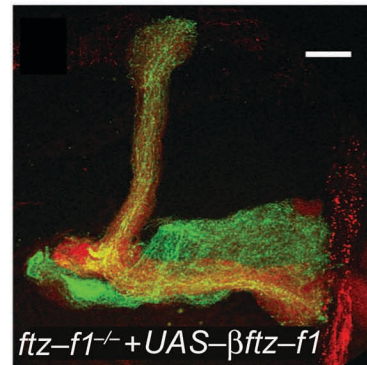
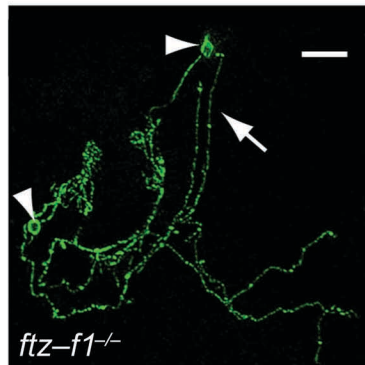
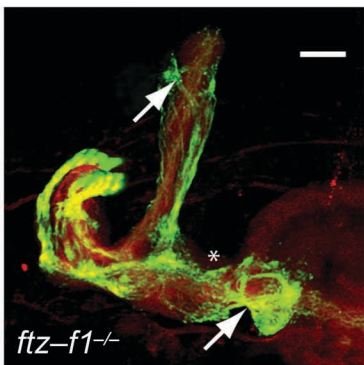
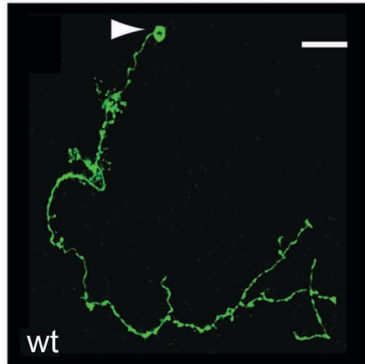
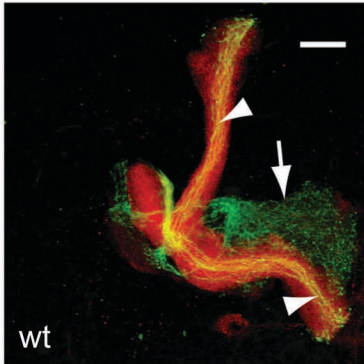
35. Mehren, J.E., Ejima, A. & Griffith, L.C. Unconventional sex: fresh approaches to courtship learning. *Curr Opin Neurobiol* 14, 745-750 (2004).
36. Davis, R.L. Olfactory memory formation in *Drosophila*: from molecular to systems neuroscience. *Annu Rev Neurosci* 28, 275-302 (2005).
37. Gonzy-Treboul, G., Lepesant, J.A. & Deutsch, J. Enhancer-trap targeting at the Broad-Complex locus of *Drosophila melanogaster*. *Genes Dev* 9, 1137-1148 (1995).
38. Nicolai, M., Lasbleiz, C. & Dura, J.M. Gain-of-function screen identifies a role of the Src64 oncogene in *Drosophila* mushroom body development. *J Neurobiol* 57, 291-302 (2003).
39. Robertson, H.M., *et al.* A stable genomic source of P element transposase in *Drosophila melanogaster*. *Genetics* 118, 461-470 (1988).
40. Engels, W.R., Johnson-Schlitz, D.M., Eggleston, W.B. & Sved, J. High-frequency P element loss in *Drosophila* is homolog dependent. *Cell* 62, 515-525 (1990).
41. Talbot, W.S., Swyryd, E.A. & Hogness, D.S. *Drosophila* tissues with different metamorphic responses to ecdysone express different ecdysone receptor isoforms. *Cell* 73, 1323-1337 (1993).
42. Yussa, M., Lohr, U., Su, K. & Pick, L. The nuclear receptor Ftz-F1 and homeodomain protein Ftz interact through evolutionarily conserved protein domains. *Mech Dev* 107, 39-53 (2001).
43. Parker, L., Ellis, J.E., Nguyen, M.Q. & Arora, K. The divergent TGF-beta ligand Dawdle utilizes an activin pathway to influence axon guidance in *Drosophila*. *Development* 133, 4981-4991 (2006).
44. Brummel, T., *et al.* The *Drosophila* activin receptor baboon signals through dSmad2 and controls cell proliferation but not patterning during larval development. *Genes Dev* 13, 98-111 (1999).
45. Jensen, P.A., Zheng, X., Lee, T. & O'Connor, M.B. The *Drosophila* Activin-like ligand Dawdle signals preferentially through one isoform of the Type-I receptor Baboon. *Mech Dev* 126, 950-957 (2009).

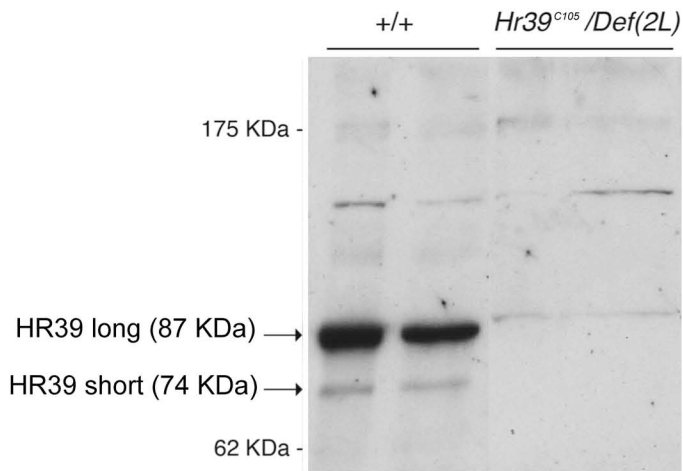
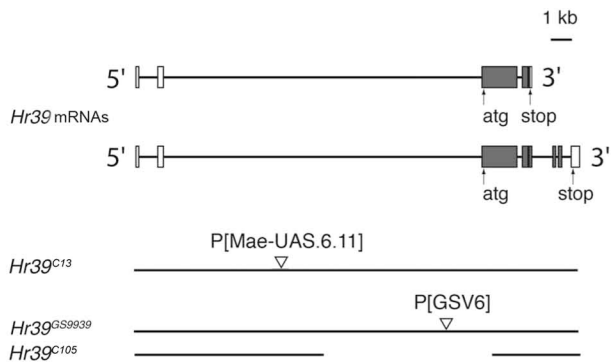
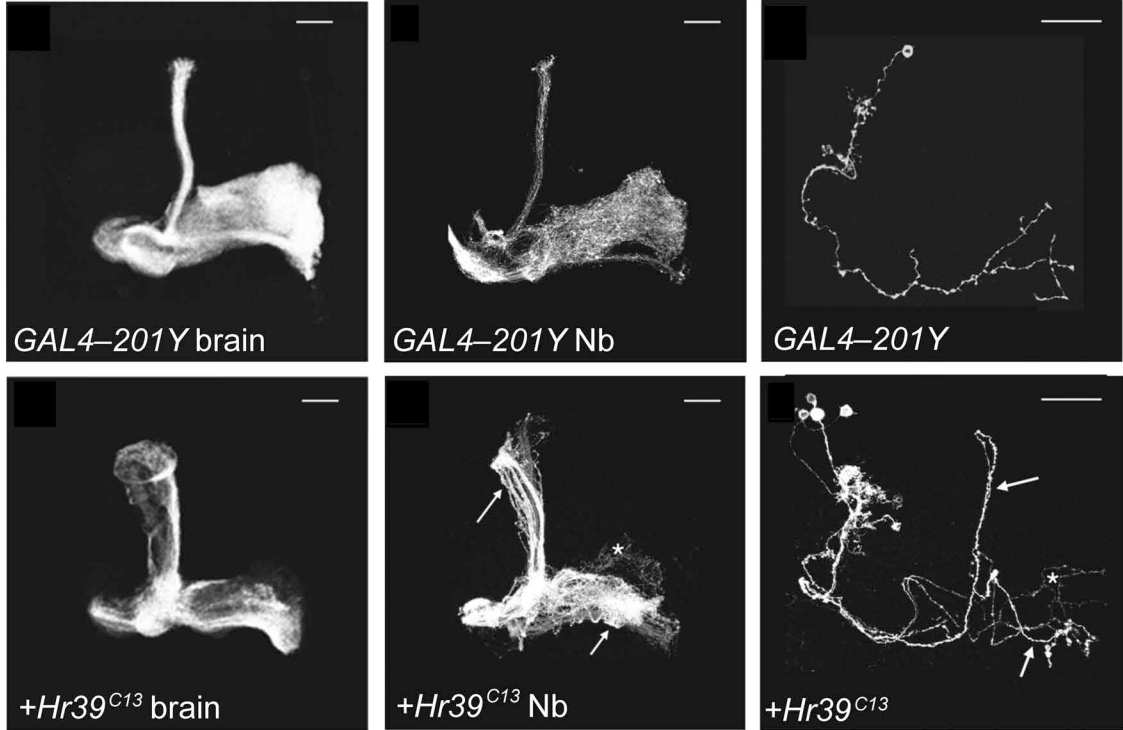
## Supplementary Information Titles

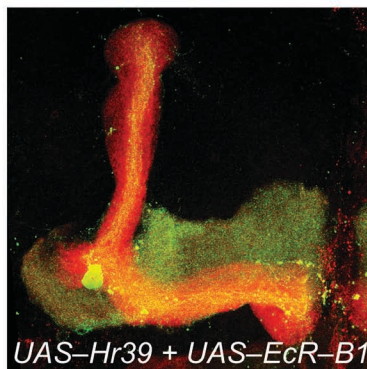
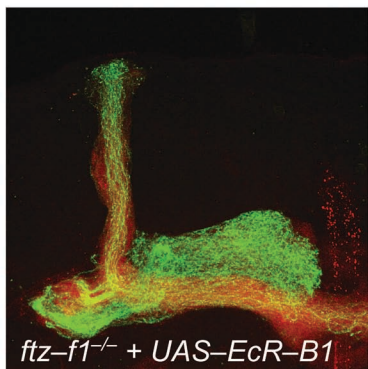
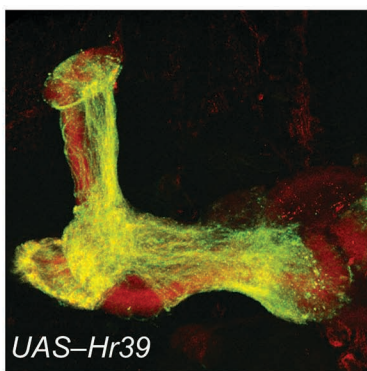
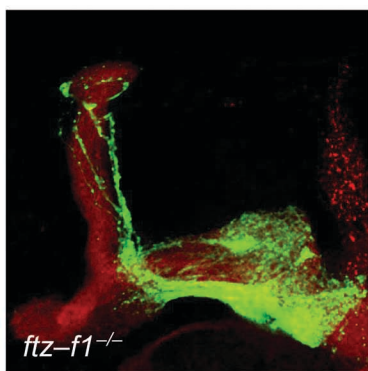
**Journal:** Nature Neuroscience

<b>Article Title:</b>	<i>ftz-fl</i> and <i>Hr39</i> opposing roles on <i>EcR</i> expression during <i>Drosophila</i> mushroom body neuron remodeling (NN-A29761B)
<b>Corresponding Author:</b>	Jean-Maurice Duram

Supplementary Item & Number (add rows as necessary)	Title or Caption
Supplementary Figure 1	FTZ-F1 expression in mushroom body $\gamma$ neurons
Supplementary Figure 2	Only $\gamma$ neurons appear affected by HR39 ectopic/over-expression in adult mushroom body neurons
Supplementary Figure 3	$\alpha\beta$ neurons do not appear affected by HR39 over-expression
Supplementary Figure 4	HR39 ectopic expression blocks pruning during development
Supplementary Figure 5	Cell fate of adult un-pruned $\gamma$ neurons is not changed
Supplementary Figure 6	Un-pruned $\gamma$ neurons are FASII positives
Supplementary Figure 6bis	Un-pruned $\gamma$ neurons are FASII positives (bis)
Supplementary Figure 7	Pruning defects of <i>babo</i> <sup>-/-</sup> are not rescued by forced expression of $\beta$ -FTZ-F1 in an <i>Hr39</i> <sup>-/-</sup> context
Supplementary Figure 8	Over-expression of HR39 and FTZ-F1 does not depend on <i>babo</i> activity in $\gamma$ neurons
Supplementary Figure 9	ECR-B1 expression quantification in different backgrounds
Supplementary Figure 10	HR39 over-expression in larval brains does not modify <i>babo<sub>a</sub></i> RNA levels
Supplementary Figure 11	<i>Hr39</i> <sup>-/-</sup> rescues <i>ftz-fl</i> <sup>-/-</sup> pruning mutant phenotypes
Supplementary Figure 12	Forced expression of HR39 in adult $\gamma$ neurons
Supplementary Figure 13	Cell fate of adult $\alpha\beta$ neurons over-expressing FTZ-F1 is not changed
Supplementary Figure 14	FTZ-F1 and HR39 bind to a common site upstream of the <i>EcR-B1</i> transcription start site
Supplementary Figure 15	A model for EcR-B1 activation in mushroom body neuron remodeling
Supplementary Figure 16	HR39 is expressed on adult heads

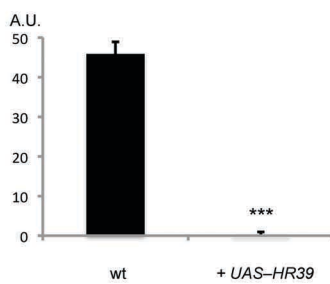
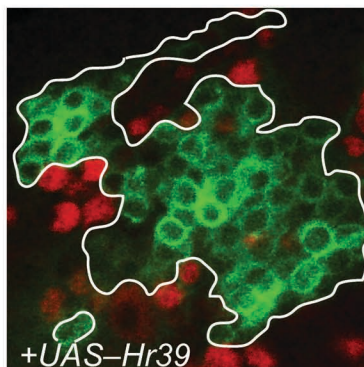
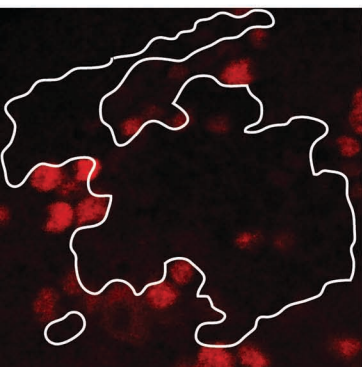
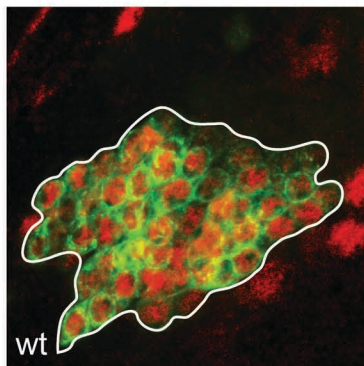
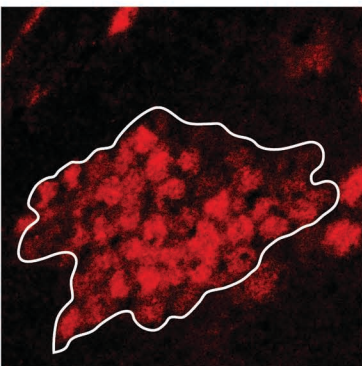
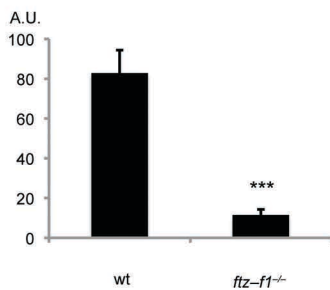
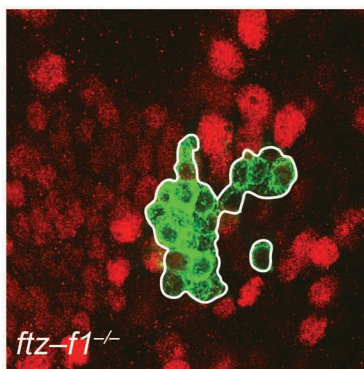
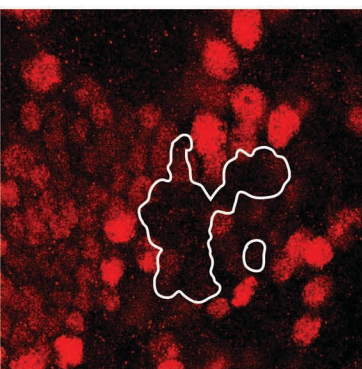
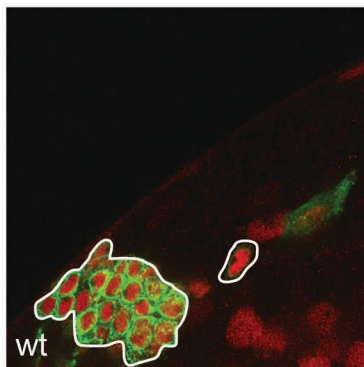
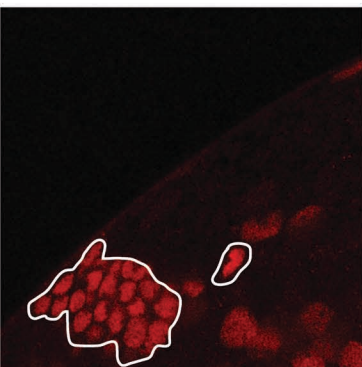


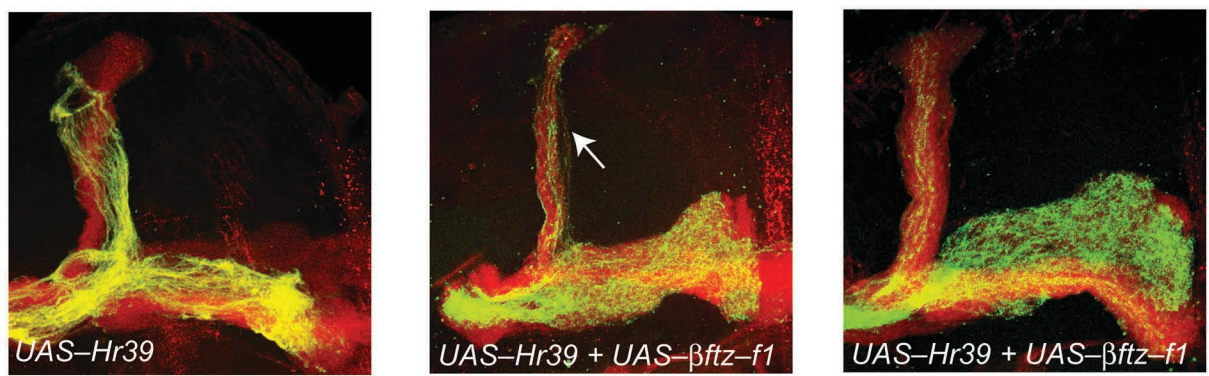
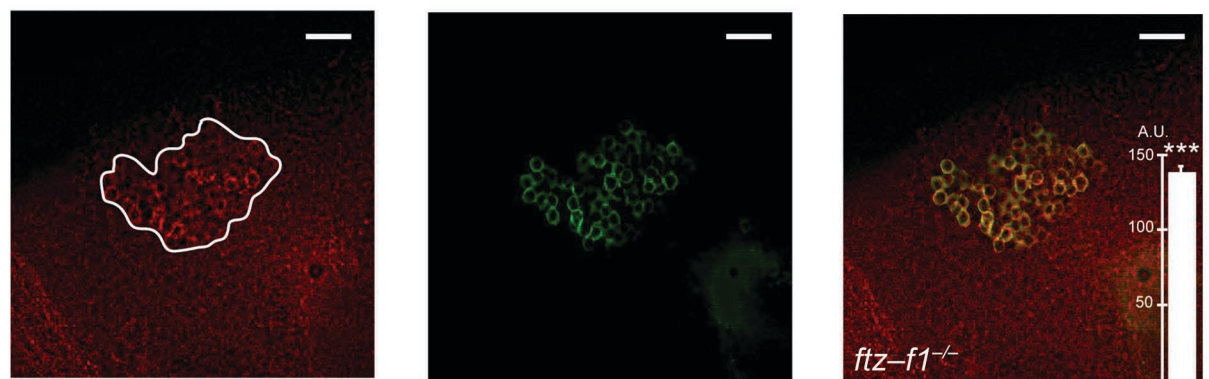
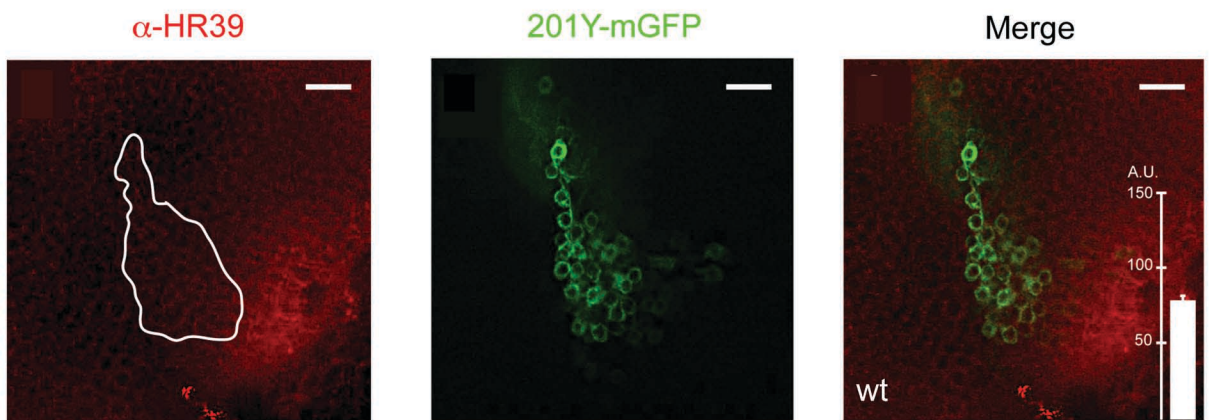
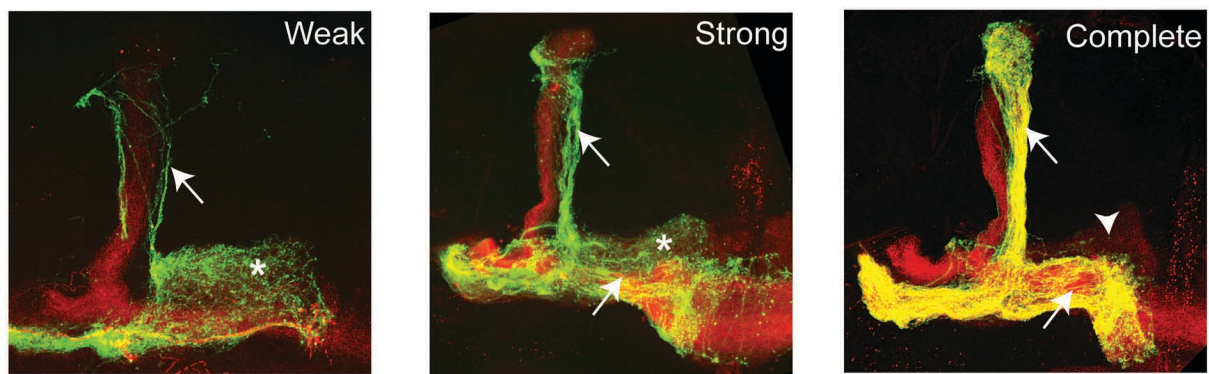


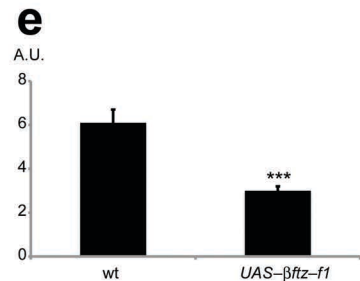
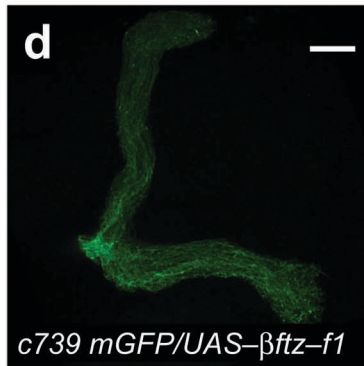
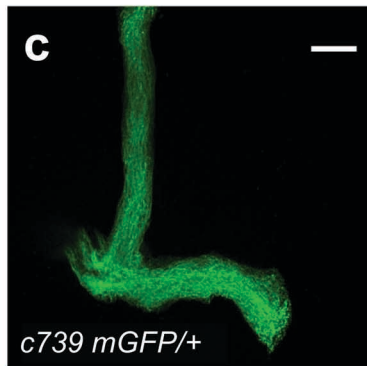
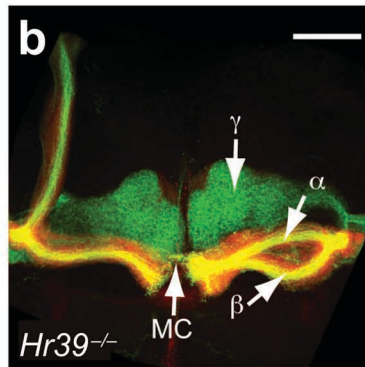
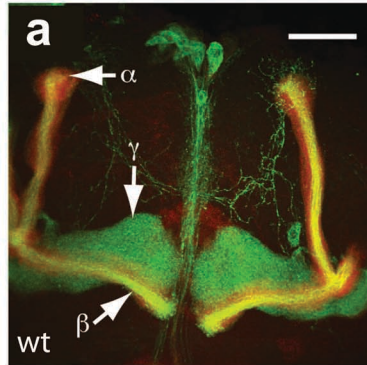


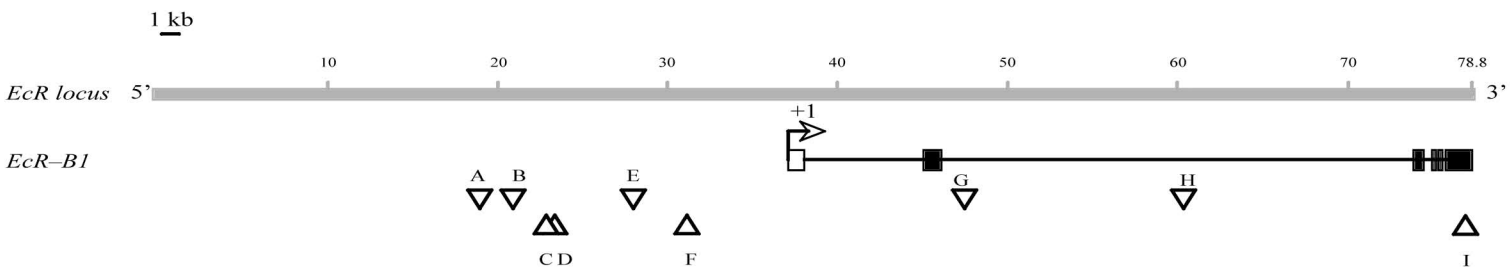
$\alpha$ -ECR-B1

Merge









YCAAGGYCR    Y = T + C  
 R = G + A

Site	Sequence	Occurrence	Localization
A	CCAAGGTCA	1	-18.2 kb
B, D	TCAAGGTCA	2	-16.1 kb (B) and -13.6 kb (D)
E	TCAAGGTCG	1	-8.8 kb
C, G, H, I	TCAAGGCCA	4	-14 kb (C), +10 kb (G), +23 kb (H) and +39.2 kb (I)
	TCAAGGCCG	Absent	-
	CCAAGGTCG	Absent	-
F	CCAAGGCCG	1	-6.1 kb

